

# Interpretation of Myoelectric Power Spectra: A Model and Its Applications

LARS H. LINDSTRÖM, MEMBER, IEEE, AND ROBERT I. MAGNUSSON, SENIOR MEMBER, IEEE

**Abstract**—Some essential elements of a mathematical model describing the power spectrum of myoelectric signals are presented. The influences of electrode configuration and of biological parameters such as muscle-fiber radius, action-potential conduction velocity, spread of synapses over the innervation zone, number of fibers per motor unit, and electrode-to-muscle distance are expressed in terms of filter functions modifying the shape of the power spectrum of the generator signal. Signal processing for parameter identification is described and results are listed. A few applications are discussed.

## INTRODUCTION

**E**LECTROMYOGRAPHY (EMG) is the art of describing myoelectric signals. These signals are the electric manifestation of the excitation process preceding the mechanical contraction in (striated) muscles. The myoelectric signal, observed with surface electrodes or coaxial needle electrodes, is composed of so-called action potentials originating from the individual muscle fibers.

The fibers of the muscle are functionally organized in subgroups, so-called motor units. The activity of each unit is controlled by a motoneuron located in the spinal cord with its axon extending to the muscle. At the muscle the axon branches into terminal nerve endings, each of which innervates a muscle fiber via a synapse, the neuromuscular junction. From the innervation point action potentials propagate in both directions along the muscle fiber. The scattered locations over the innervation zone cause a time dispersion of the action potentials with respect to a fixed recording position. The scattering also causes the fibers of a particular motor unit to be intermingled with fibers from several other units.

The muscle contractile force is modulated by varying the repetition rate of activating motoneuron pulses, typically some 10 Hz, and by varying the recruitment of motor units. At low levels of contraction few units are active. With increasing demand of force the repetition rate increases and new units are recruited.

The main concern in clinical EMG investigations is the motor-unit signal, which is characterized by its amplitude, duration, and number of so-called phases (i.e., oscillations). Such investigations are generally restricted to the analysis of signals obtained at low levels of contraction. Even at moderate contraction levels, so many motor units are active that the observed signal has the character of random noise. However, there is still a considerable amount of information in the myoelectric signal. The noisy appearance of the signal suggests methods of random signal analysis for extraction of this infor-

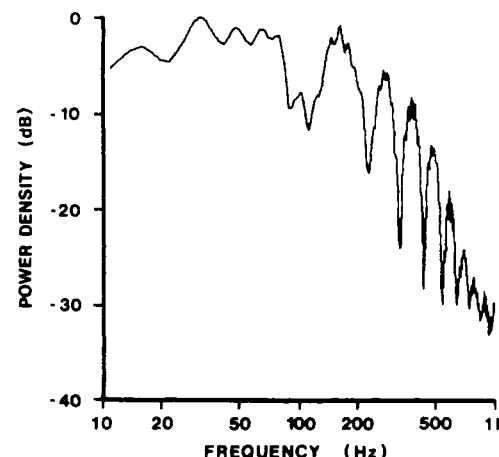


Fig. 1. Power spectrum of myoelectric signal from the biceps brachii muscle (single motor unit) obtained with a bipolar surface electrode of plate separation  $2d = 4$  cm.

mation. One such method is power spectrum analysis, the subject of this paper. An example of a myoelectric power spectrum is shown in Fig. 1.

In order to interpret the myoelectric signal in terms of anatomical and physiological parameters a model describing the power spectrum of these signals has been developed [1], and later reformulated and extended [2]–[6]. Some essential elements of this model are summarized in this paper.

## THEORY

Consider a muscle consisting of individual muscle fibers functionally organized in motor units and lined up in one and the same direction, the  $x$  axis. The fibers and the extracellular fluid constitute the medium in which the myoelectric signals are spread by volume conduction. We shall assume the medium to be isotropic, homogeneous, and to have a linear current-voltage characteristic.

### Muscle Action-Potential Transform

The muscle fibers are described as long cylinders of radius  $a$ . The action potentials propagate with velocity  $v$  in both directions from the innervation point at coordinate  $x_n$ . Since our intended application of the model is for power spectrum analysis we prefer to consider the Fourier transform of the action potential, i.e., an infinite sum of travelling waves having the amplitudes

$$\int_{-\infty}^{\infty} \phi_a(t - x_0/v) \exp(-j\omega t) dt = \psi_a(j\omega) \exp(-j\omega x_0/v). \quad (1)$$

Manuscript received July 1, 1976; revised October 2, 1976.

L. H. Lindström is with the Department of Clinical Neurophysiology, Sahlgren Hospital, and the Department of Applied Electronics, Chalmers University of Technology, Göteborg, Sweden.

R. I. Magnusson is with the Department of Applied Electronics, Chalmers University of Technology, Göteborg, Sweden.

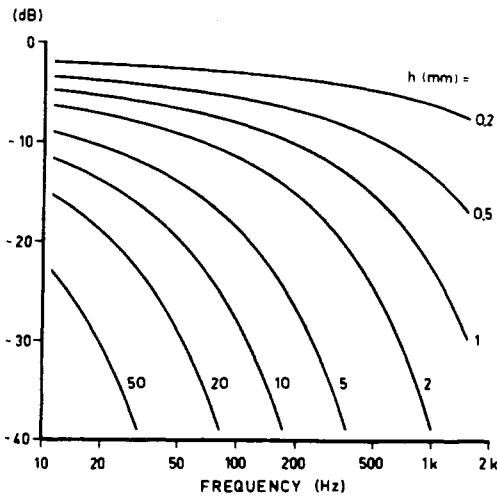


Fig. 2. Distance-damping function  $K_0^2(\omega h/v)/K_0^2(\omega a/v)$  as a function of frequency. Parameter values are: fiber radius  $a = 50 \mu\text{m}$  and conduction velocity  $v = 4 \text{ m/s}$ .

Here,  $\phi_a(t - x_0/v)$  is the time-dependent action potential at the fiber surface recorded at  $x = x_0$  and  $\omega$  denotes angular frequency.

#### Distance Filtering Function

Since the time constant of the medium is extremely short compared with any other characteristic time involved, we can calculate the Fourier components  $\psi(j\omega)$  of the electric field outside the fiber by solving Laplace's equation. For the geometry of an infinitely long cylinder we find [1], [2]

$$\psi(j\omega) = \psi_a(j\omega) \exp(-j\omega x_0/v) K_0(\omega h/v) / K_0(\omega a/v) \quad (2)$$

where  $K_\nu(\xi)$  is the modified Bessel function of the second kind, order  $\nu$ , and argument  $\xi$ , and  $h$  denotes the radial distance from the center of the fiber to the point of measurement.

The filtering function  $K_0(\omega h/v)/K_0(\omega a/v)$  is plotted in logarithmic scales in Fig. 2. It has the character of a low-pass filter, the cutoff frequency of which is inversely proportional to the observation distance  $h$ . A plot of the filtering function versus distance gives information on the extension of the region from which signals of significant strength can be obtained [1], [7].

In virtually all practical situations the influence of non-infinitely long fibers and innervation-point positions will modify the filtering function. An alternative formulation involving integration of signal contributions along the muscle fiber is then more accurate [1], [2]. In spite of this, the Bessel functions according to (2) will be used for convenience in subsequent calculations.

#### Electrode Filtering Effects

The influence of the electrodes used for leading off the myoelectric signal is described by the electrode transfer function  $F_{el}(j\omega)$ , defined as follows:

$$F_{el}(j\omega) \triangleq \Delta\psi_{el}(j\omega)/\psi(j\omega). \quad (3)$$

Here,  $\Delta\psi_{el}$  is the Fourier transform of the potential difference between the two electrode lead-off surfaces, and the subscript "el" stands for the electrode type, e.g., coaxial needle electrode ("coax"), bipolar surface electrode ("bipol"), etc.

We shall first give some indication of how the concentric needle electrode used in clinical practice affects the spectrum of the myoelectric signal. The interface impedance between cannula and tissue is usually quite large, and the insertion of the needle does not seriously affect the potential distribution in the tissue [8]. Accordingly, we put the cannula potential equal to the average potential, obtained by integration of the preexisting potentials at the cannula surface. For simplicity we consider a concentric needle electrode perpendicular to the muscle fiber and inserted a depth  $h_0$  into the tissue. The elliptic shape of the electrode tip—yielded by the oblique cut of the needle—is also, for simplicity, replaced by a circular one. The difference between the Fourier components of the center electrode and the cannula shield of radius  $R$  is [2]

$$\Delta\psi_{\text{coax}}(j\omega) = \frac{\psi_a(j\omega)}{K_0(\omega a/v)} \left\{ K_0(\omega h/v) \exp(-j\omega x_0/v) - \frac{1}{2\pi h_0} \int_h^{h+h_0} d\xi \int_0^{2\pi} d\beta K_0(\omega \xi/v) \cdot \exp(-j\omega[x_0 - R \cos \beta]/v) \right\}. \quad (4)$$

The filtering function of the concentric needle electrode is thus found to be

$$F_{\text{coax}}(j\omega) = 1 - \frac{J_0(\omega R/v)}{h_0 K_0(\omega h/v)} \int_h^{h+h_0} K_0(\omega \xi/v) d\xi \quad (5)$$

where  $J_0(\omega R/v)$  is the Bessel function of the first kind and order zero. The insertion depth of the needle is always much larger than the cannula radius, and the function  $J_0(\omega R/v)$  can be assigned the value unity in most approximate expressions of the filtering function. A number of such approximations, valid for different situations, can be derived [2]; in essence we find that

$$F_{\text{coax}}(j\omega) \approx \frac{\omega h_0}{2v} \cdot \frac{K_1(\omega h/v)}{K_0(\omega h/v)}, \quad \omega h_0/v \ll 1 \quad (6a)$$

and

$$F_{\text{coax}}(j\omega) \approx 1, \quad \omega h_0/v \gg 1. \quad (6b)$$

The filtering function  $F_{\text{coax}}(j\omega)$  according to (5) is that of a high-pass filter, the maximum low-frequency slope of which is 6 dB/octave, obtained for small values of the insertion depth and large values of the needle-to-fiber distance. All other combinations of parameter values yield slopes less than 6 dB/octave. This moderate influence of the needle electrode on the recorded myoelectric signal has experimental support in the findings [9], [10] that the motor-unit potential duration is essentially the same for monopolar and concentric needle electrodes.

With slight modifications, the expressions for the concentric needle electrode filtering function are also valid for describing the filtering effect of intramuscular wire electrodes.

For bipolar electrodes (surface as well as differential needle electrodes), with the electrode plates lined up in the direction of the muscle fibers and having a plate center separation of  $2d$ , the filtering function is easily calculated by taking the difference in potential at coordinates  $x_0 - d$  and  $x_0 + d$ , respectively. The Fourier transform of this potential differ-

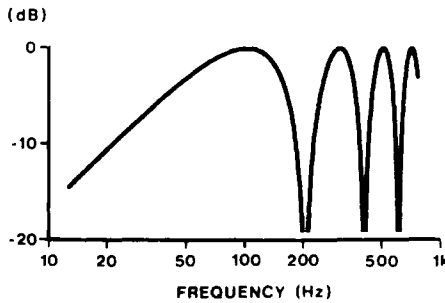


Fig. 3. Surface electrode filter function  $|F_{\text{bipol}}(j\omega)|^2$ . Parameter values are: electrode plate separation  $2d = 2$  cm and conduction velocity  $v = 4$  m/s.

ence is [1], [2]

$$\Delta\psi_{\text{bipol}}(j\omega) = \psi_a(j\omega) \frac{K_0(\omega h/v)}{K_0(\omega a/v)} \left[ \exp\left(-j\omega \frac{x_0 - d}{v}\right) - \exp\left(-j\omega \frac{x_0 + d}{v}\right) \right] \quad (7)$$

and the bipolar electrode filter function is found to be [1], [2]

$$F_{\text{bipol}}(j\omega) = 2j \sin(\omega d/v). \quad (8)$$

The influence of the bipolar electrode on the myoelectric signal power spectrum is shown in Fig. 3. As noticed by several authors [8], [11], [12] the filter function behaves like a differentiating filter that adds a positive slope of 6 dB/octave to the spectrum in the low-frequency region. The differentially coupled bipolar electrode has an additional property: it introduces so-called dips into the spectrum at those frequencies where the sine function is equal to zero, i.e., at

$$\omega = n\pi v/d \quad (9)$$

$n$  being an integer (cf. Fig. 1).

Given the electrode size we can thus determine the conduction velocity from the following formula:

$$v = 2d f_{\text{dip}}/n, \quad n = 1, 2, \dots \quad (10)$$

where  $f_{\text{dip}}$  is the frequency of the dip of order  $n$ . The dip-analysis method permits quite accurate measurements of the conduction velocity of action potentials obtained with surface electrodes.

#### Motor-Unit Signal

The properties of the motor-unit signal can be calculated from the time series of an ensemble. For the moment we focus our attention on a single motor-unit potential made up of the contributions of  $N$  fibers. The time dispersion of the individual action potentials in the motor-unit signal has its origin in: a) different travelling times of variance  $\sigma_n^2$  of the triggering impulses in the motor nerve endings after branching, b) differences in the delay times of variance  $\sigma_{\tau_0}^2$  in the synapses between the nerve endings and the muscle fibers, c) the geometrical spread of variance  $\sigma_x^2$  of the synapses in the fiber direction (i.e., spread in  $x_n$ ), and d) the dispersion of the action-potential conduction velocities, the variance of which is denoted by  $\sigma_v^2$ . In what follows, these processes are considered to be mutually independent. Thus the total variance

$\sigma_\tau^2$  in arrival times of the single-fiber contributions to the motor-unit signal is

$$\sigma_\tau^2 = \sigma_n^2 + \sigma_{\tau_0}^2 + (\sigma_x/v_0)^2 + (\sigma_v/v_0)^2 (x_0/v_0)^2 \quad (11a)$$

where  $v_0$  is the average action-potential conduction velocity, and the average of  $x_n$  is taken to be zero. Of all the dispersing processes listed above, the most dominating influence generally arises from the spread of innervation points, i.e., from  $\sigma_x$  [13]. In the evaluation of experiments we will thus use the approximation

$$\sigma_\tau^2 \approx \sigma_x^2/v_0^2. \quad (11b)$$

Let the Fourier transform of the signal of the  $n$ th fiber of the motor unit be

$$\psi_n = \psi_a(j\omega) \frac{K_0(\omega h/v)}{K_0(\omega a/v)} F_{e1}(j\omega) \quad (12)$$

where  $a$ ,  $v$ , and  $h$  now are stochastic variables assumed to be mutually independent. The phase factor  $\exp(-j\omega x_0/v)$  is combined with that of the time delays at the innervation region to yield the stochastic factor  $\exp(-j\omega \tau_n)$ , where  $\tau_n$  is the total time delay which is assumed to be independent of the other variables. Without loss of generality the expected value of  $\tau_n$  is set equal to zero. For convenience, the probability density of  $\tau_n$  is assumed to be an even function with variance  $\sigma_\tau$ , as given by (11a, b).

The expressions for the Fourier transform and the power spectrum of the motor-unit signal can be formally written as expected values  $\psi_{\text{mu}}(j\omega)$  and  $W_{\text{mu}}(\omega)$ , with variances  $\sigma_\psi^2(j\omega)$  and  $\sigma_W^2(\omega)$ .

From Broman and Lindström [3] we take

$$\psi_{\text{mu}}(j\omega) = N E[\psi_n] C(\omega) \quad (13)$$

$$\sigma_\psi^2(j\omega) = N E[\psi_n^2] C(2\omega) - N E^2[\psi_n] C^2(\omega) \quad (14)$$

$$W_{\text{mu}}(\omega) = N E[\psi_n \psi_n^*] + N(N-1) E[\psi_n] E[\psi_n^*] C^2(\omega) \quad (15)$$

and

$$\begin{aligned} \sigma_W^2(\omega) = & N E[\psi_n^2 \psi_n^{*2}] \\ & + 2N(N-1) \{ E[\psi_n^2 \psi_n^*] E[\psi_n^*] \\ & + E[\psi_n \psi_n^{*2}] E[\psi_n] \} C^2(\omega) \\ & + N(N-2) E^2[\psi_n \psi_n^*] \\ & + N(N-1) E[\psi_n^2] E[\psi_n^{*2}] C^2(2\omega) \\ & + 2N(N-1)(N-4) E[\psi_n \psi_n^*] E[\psi] E[\psi_n^*] C^2(\omega) \\ & + N(N-1)(N-2) \{ E[\psi_n^2] E^2[\psi_n^*] \\ & + E^2[\psi_n] E[\psi_n^{*2}] \} C(2\omega) C^2(\omega) \\ & + N(N-1)(-4N+6) E^2[\psi_n] E^2[\psi_n^*] C^4(\omega) \end{aligned} \quad (16)$$

where  $\psi_n^*$  is the complex conjugate of  $\psi_n$ . In the above equations we have used the characteristic function  $C(\omega)$  of the even distribution of arrival times  $\tau_n$ . Thus a Gaussian density with zero mean and standard deviation  $\sigma_\tau$  yields

$$C(\omega) = \exp(-\omega^2 \sigma_\tau^2/2). \quad (17)$$

For mathematical convenience, such a density will be assumed in what follows. On the further assumption that  $a$ ,  $v$ , and  $h$  are constant, i.e., that the single-fiber signals have

identical shape, we obtain [3] the following expressions valid for electrode locations well outside the motor unit and far away from the innervation zone. The Fourier component is

$$\psi_{mu}(j\omega) = \psi_a(j\omega) \frac{K_0(\omega h/v)}{K_0(\omega a/v)} F_{el}(j\omega) N \exp\left(-\frac{\omega^2 \sigma_r^2}{2}\right) \quad (18)$$

with variance

$$\sigma_\psi^2(j\omega) = \psi_a^2(j\omega) \frac{K_0^2(\omega h/v)}{K_0^2(\omega a/v)} F_{el}^2(j\omega) N \{ \exp(-2\omega^2 \sigma_r^2) - \exp(-\omega^2 \sigma_r^2) \} \quad (19)$$

and the power spectrum is

$$W_{mu}(\omega) = \psi_a(j\omega) \psi_a^*(j\omega) \frac{K_0^2(\omega h/v)}{K_0^2(\omega a/v)} F_{el}(j\omega) F_{el}^*(j\omega) \cdot N \{ 1 + (N-1) \exp(-\omega^2 \sigma_r^2) \} \quad (20)$$

with variance

$$\sigma_W^2(\omega) = \psi_a^2(j\omega) \psi_a^{*2}(j\omega) \frac{K_0^4(\omega h/v)}{K_0^4(\omega a/v)} F_{el}^2(j\omega) F_{el}^{*2}(j\omega) N \cdot (N-1) \{ 1 - \exp(-\omega^2 \sigma_r^2) \}^2 \{ 1 + 2(N-1) \exp(-\omega^2 \sigma_r^2) + \exp(-2\omega^2 \sigma_r^2) \} \quad (21)$$

For the subsequent treatment of whole-muscle signals we also need the expression for the power spectrum of signals obtained with electrodes located within the motor-unit territory. In this case we have to take into account the stochastic nature of  $h$ . We assume that the electrode filtering function  $F_{el}(j\omega)$  is only weakly dependent on the distance  $h$ . The dependence then mainly enters through the modified Bessel function  $K_0(\omega h/v)$ , which we expand in a Taylor series around the expected value  $h_0 = E[h_n]$ . Neglecting terms of an order higher than two we find

$$E[K_0(\omega h_n/v)] \approx K_0(\omega h_0/v) + \frac{1}{2} \sigma_h^2 \left[ \frac{d^2}{dh^2} K_0(\omega h/v) \right]_{h=h_0} \quad (22)$$

where  $\sigma_h^2$  is the variance of  $h_n$ . Equations (12), (15), and (22) yield the following expression for the motor-unit signal power spectrum valid for small as well as large values of the electrode to motor-unit distance:

$$W_{mu}(\omega) = \psi_a(j\omega) \psi_a^*(j\omega) \frac{F_{el}(j\omega) F_{el}^*(j\omega)}{K_0^2(\omega a/v)} N \cdot \left\{ K_0^2(\omega h_0/v) [1 + (N-1) \exp(-\omega^2 \sigma_r^2)] + \left( \frac{\omega \sigma_h}{v} \right)^2 \left( \left[ K_0^2(\omega h_0/v) + \frac{K_0(\omega h_0/v) \cdot K_1(\omega h_0/v)}{\omega h_0/v} \right] \cdot [1 + (N-1) \exp(-\omega^2 \sigma_r^2)] + K_1^2(\omega h_0/v) \right) \right\} \quad (23)$$

The influence of the stochastic variations in action-potential conduction velocity can be described in a similar manner [3].

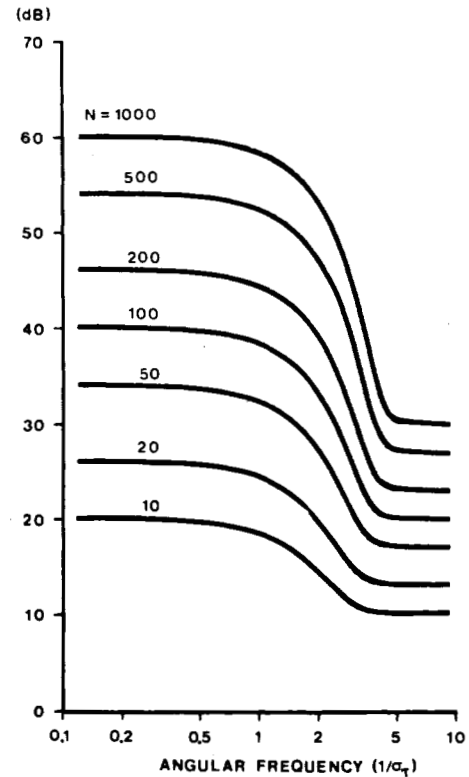


Fig. 4. Equivalent filter function of dispersed signal summation within a motor unit, obtained from (20) after normalization. Parameter  $N$  is the number of signal sources (fibers).

The most prominent effect of the summation of dispersed signals is that of low-pass filtering. The modifying effect of the summation is illustrated in Fig. 4, where power spectra of motor-unit signals according to (20), normalized with respect to the power spectrum of the single-fiber signal, are plotted for a various number of sources. It should be noted that the assumed Gaussian density of fiber-signal arrival times in all probability yields lower values of high-frequency energy than does the actual density function.

In the low-frequency region the contributions add linearly because of preserved coherence, i.e., preserved relative phase of the Fourier components. At the frequency

$$\omega_0 \approx 1/\sigma_r \quad (24)$$

a gradual decrease in coherence becomes apparent, yielding an increased roll-off of the equivalent low-pass filter up to the frequency

$$\omega_1 \approx \omega_0 \sqrt{\ln N} \quad (25)$$

above which a square-law summation yields constant values of the filter function (cf. Fig. 1).

The difference between the low- and high-frequency levels of the filter function is proportional to the number of fibers in the motor unit. Thus small muscles, which generally have fewer fibers per motor unit, will show power spectra containing relatively higher amounts of high-frequency activity than will muscles with large motor units. Further effects of muscle size on the observed power spectrum will be treated below.

Some features of the variance estimates should also be considered. From (15) and (16) we can conclude that the

variance of the power spectrum, normalized with respect to the square of the power spectrum, is a function which increases from zero at low frequencies to the value  $(N-1)/N$  as the frequency goes to infinity. In practice the final value is reached at the frequency  $\omega_1$  defined in (25). Interpretation of EMG findings in the frequency region of square-law summation should thus be performed with great care. In contrast to this, it might be argued that the summation of motor-unit signals into the whole-muscle signal will somewhat reduce the normalized variance.

### Whole-Muscle Signal

In most measurements of myoelectric activity at moderate and high contraction levels, motor units in the whole muscle, and even in adjacent ones, contribute to the observed signal. Analytically, the summation of motor-unit signals is performed by integration over the muscle with the distance-dependent filtering functions as weighting functions. Let us assume that the electrode (intramuscular needle or surface type) can be regarded as small compared to the size of the muscle, and choose the semicircular strip  $\pi \cdot h \cdot dh$  as the element of integration. Let us further assume that the motor-unit contributions are mutually independent and thus add as energies. Under the assumptions listed, the total signal power spectrum  $W_f(\omega)$  can be written as follows:

$$W_f(\omega) = \int_{h_{\min}}^{h_{\max}} W_{\text{mu}}(\omega) N^{-1} a^{-2} h \, dh. \quad (26)$$

Here,  $W_{\text{mu}}(\omega)$  is given by (23) and  $(N\pi a^2)^{-1}$  is the mean density of motor units. The integration limits  $h_{\min}$  and  $h_{\max}$  are the distances from the observation point to the centers of the closest and the most remote active motor units, respectively. Evaluation of (26) yields [4]

$$W_f(\omega) = \frac{\psi_a(j\omega)\psi_a^*(j\omega)F_{e1}(j\omega)F_{e1}^*(j\omega)}{2(\omega a/v)^2 K_0^2(\omega a/v)} \cdot \{H(s, Q, u_{\min}) - H(s, Q, u_{\max})\} \quad (27)$$

where, for shortness of notation, we have put

$$H(s, Q, u) \triangleq Q(1+s^2)u^2 [K_1^2(u) - K_0^2(u)] + s^2 Q K_0^2(u) + s^2 u^2 [K_0^2(u) + \frac{2}{u} K_0(u)K_1(u) - K_1^2(u)] \quad (28)$$

$$s \triangleq \omega \sigma_h / v \quad (29)$$

$$u \triangleq \omega h_0 / v \quad (30)$$

and

$$Q \triangleq 1 + (N-1) \exp(-\omega^2 \sigma_f^2). \quad (31)$$

The lower limit of integration  $u_{\min} = \omega h_{\min}/v$  can be related to the mean size of the motor units. The expression for the most probable distance between the closest motor-unit center point and the tip of a randomly inserted needle electrode [4] is

$$h_{\min} = \beta a N^{1/2} \quad (32)$$

where  $\beta$  is a parameter proportional to the average intercenter distances between active motor units. The lowest value of  $\beta$ , approximately equal to 0.45, is obtained (as with honey bees) for a close-packed structure of hexagonal units. The param-

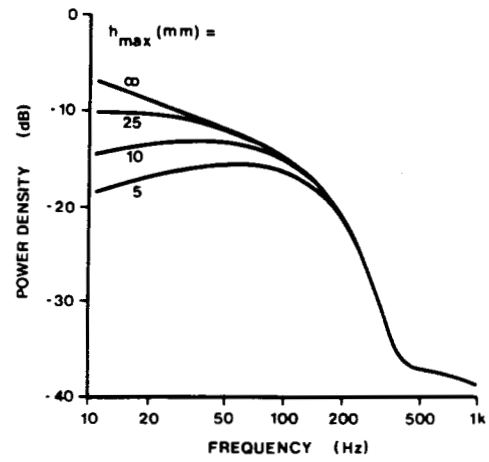


Fig. 5. Influence of parameter  $h_{\max}$  on theoretical power spectra of whole-muscle signals derived with monopolar intramuscular electrodes. Parameter values are: standard deviation of motor-unit signal temporal dispersion  $\sigma_f = 1$  ms, conduction velocity  $v = 4$  m/s, fiber radius  $a = 20$   $\mu\text{m}$ , number of fibers in motor units  $N = 200$ ,  $\beta = 1.5$ , and  $\eta = 0.2$ .

eter  $\beta$  mainly influences the high-frequency part of the power spectrum: large values of  $\beta$  yield a more rapid roll-off than do low values.

The standard deviation  $\sigma_h$  can also be expressed as a function of the mean values of fiber radius and number of motor-unit fibers. For a Gaussian distribution of fibers over the muscle cross section we find that

$$\sigma_h = a \left( \frac{N}{2\eta} \right)^{1/2} \quad (33)$$

where  $\eta$  is the motor-unit filling factor, i.e., the inverse value of the number of intermingled motor units. The parameter  $\eta$  has a comparatively weak influence on the power spectrum. An increased mixing of units increases the high-frequency content of the spectrum slightly.

Among the remaining parameters of (27), muscle size, expressed by the distance  $h_{\max}$ , has a pronounced effect on the power spectrum. Increasing values of  $h_{\max}$  give energy increases in the low-frequency region, as illustrated in Fig. 5. Correspondingly, excessive low-frequency power densities in intramuscular myoelectric recordings are often an indication of cross talk from adjacent muscles. The muscle-size influence on the spectrum is consistent with, in addition to the effects of signal summation, the observation [14]–[17] that small muscles have signals whose spectra are shifted to the high-frequency region.

The shape of the total myoelectric signal power spectrum (equation (27)) is weakly dependent on the mean fiber radius  $a$ . The influence of muscle-fiber size on the action-potential conduction velocity [18], [19] should be remembered, although it has not been explicitly included in the equations.

In the case of extramuscular electrodes, fiber scattering  $\sigma_h$  can be neglected in comparison with electrode-to-motor-unit distances. Thus putting  $\sigma_h$  equal to zero in (27), we obtain the power spectrum of the whole-muscle signal derived with surface electrodes. The shape of this spectrum is largely determined by the same parameters as that of intramuscularly derived signals. The parameter  $h_{\min}$ , now the shortest

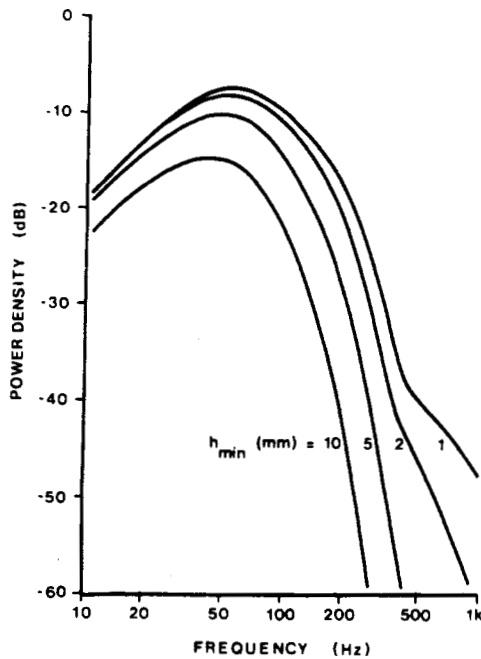


Fig. 6. Influence of parameter  $h_{\min}$  on the envelope of power spectra of whole-muscle signals derived with bipolar surface electrodes. Parameter values are: standard deviation of motor-unit signal temporal dispersion  $\sigma_T = 1$  ms, conduction velocity  $v = 4$  m/s, fiber radius  $a = 20$   $\mu$ m, number of fibers in motor units  $N = 200$ , maximum electrode-to-muscle distance  $h_{\max} = 15$  mm, and electrode plate separation  $2d = 3$  cm.

electrode-to-muscle distance, will have a more pronounced effect on the high-frequency region than was found in the case of needle electrodes. As an example, theoretical spectra for various values of  $h_{\min}$  are shown in Fig. 6.

It is interesting to note that in all expressions for the myoelectric signal power spectrum, except the one demonstrating the coaxial needle electrode influence, the frequency always appears in combination with the action-potential conduction velocity as the quotient  $\omega/v$ . The conclusion that changes in conduction velocity are always observed as translations of the spectrum along the frequency axis is of fundamental importance for understanding many experimental findings.

The source signal  $\psi_a(j\omega)$  also follows this rule. This is realized by considering the space-dependent action potential  $\Theta_a(x - vt)$  rather than the time-dependent one,  $\phi_a(t - x/v)$ . From (1), with the substitution  $z = x - vt$ , we find

$$\psi_a(j\omega) = \frac{1}{v} \int_{-\infty}^{\infty} \Theta_a(z) \exp(jz\omega/v) dz. \quad (34)$$

Recent experimental evidence indicates that, although not completely invariant,  $\Theta_a(z)/v$  is less dependent on changes in conduction velocity than is  $\phi_a(\tau)$ .

In conclusion, it should be stated that the present theory, with minor modifications, can be applied to other forms of bioelectric activity, for example that of peripheral nerves.

#### EXPERIMENTAL VERIFICATION

In order to demonstrate the myoelectric signal power spectrum model a few experiments will be described. Due to obvious experimental difficulties, direct verification of all relations constituting the model is impossible. We have chosen an alternate route for most of the experiments. Since all parameters of the model have well-defined biological meaning, we have made parameter identifications and compared results

thus obtained to previously known results obtained with histological, anatomical, and physiological methods. The parameter identification was performed digitally on logarithmically scaled data by varying parameter values until the minimum mean-square error was reached. Unless otherwise stated, power spectra were obtained by means of the fast Fourier transform.

#### Single Fiber Parameters

The action potential at the fiber surface cannot be measured *in situ* since the actual distance from the electrode to the muscle-fiber membrane is unknown. In order to investigate the influence of the distance-dependent damping according to (2) we can take as a fictive source the action potential measured at a certain (but unknown) distance  $h_1$ , say, and relate it to other action potentials measured at distances  $h_n$  of known geometric relation to  $h_1$ . From the series of ratios

$$[\psi(j\omega)]_{h_n} / [\psi(j\omega)]_{h_1} = K_0(\omega h_n/v) / K_0(\omega h_1/v) \quad (35)$$

one may estimate the distances.

Such experiments were performed [20], [21] according to the so-called single-fiber EMG technique [22], [23]. The agreement between estimated and predicted ratios was found to be reasonably good: the average deviation was close to two percent [3]. Since, for short distances, the distance-damping filtering function does not affect the spectrum too strongly, the properties of the source could also be estimated. For frequencies up to 1 kHz, it was found that the power spectrum of the source is approximately proportional to the frequency, i.e., that  $\alpha \approx 1$  in (36) below.

Based on these and other experiments, as well as on the theoretical considerations in connection with (34), we introduce the following simplified expression for the energy spectrum of the source signal:

$$\psi_a(j\omega)\psi_a^*(j\omega) = S_0 v^{-\gamma} (\omega/v)^\alpha \quad (36)$$

where  $S_0$  is constant with respect to  $v$  and  $\omega$ . Clearly, the evidence so far discussed suggests exponent values of  $\alpha \approx 1$  and  $\gamma \approx 2$ .

#### Dip Analysis

The so-called dips in the power spectra, which are predicted by the above theory to occur for differentially derived myoelectric signals, have been verified experimentally [1] and have been used to determine action-potential conduction velocities in the biceps brachii muscle [24]. The velocities found, in the range 3.5–4.8 m/s, agree well with previously published values [23], [25], which range from 2.8 to 5.9 m/s. An example of a motor-unit signal spectrum with multiple dips is given in Fig. 1.

#### Motor Unit Parameter

The parameters of the signal from a biceps brachii motor unit have been determined in one case [3]. Two hundred averaged potentials gave a low-noise recording of sufficient quality to provide the following result:  $v = 3.9$  m/s (from dip analysis),  $h_{\min} = 1.9$  mm,  $N = 160$ , and  $\sigma_T = 0.6$  ms. Accordingly, from (11b), the standard deviation  $\sigma_x$  of the motor-unit synaptic spread is approximately 2.3 mm. The quantity  $\sigma_T$  is related to the motor-unit signal duration. On statistical grounds the duration should correspond to about  $6\sigma_T$ . Data from the literature state that the duration for the biceps brachii muscle ranges from 5.7 to 10 ms [9], [26], which thus should be compared to  $6\sigma_T = 3.6$  ms.

TABLE I

Identified values of parameters in power spectra of myoelectric signals from the biceps brachii and extensor carpi radialis muscles obtained with bipolar surface electrodes at load level 1 kg. Fixed parameter values are: $h_{\max} = 5$ mm and $\alpha = 1$ . (S.E.M. is the standard error of the mean.)					
		m. biceps brachii		m. extensor carpi radialis	
		mean	S.E.M.	mean	S.E.M.
$h_{\min}$	(mm)	2.5	0.7	1.9	0.5
$\sigma_t$	(ms)	0.66	0.05	0.42	0.08
$v$	(m/s)	4.7	0.4	5.4	1.4
average error	(dB)	0.5	0.1	1.9	0.5
samples		11		6	

TABLE II

Identified values of parameters in power spectra of myoelectric signals from the biceps brachii and extensor carpi radialis muscles obtained with bipolar surface electrodes at load level 1 kg. Fixed parameter values are: $v = 4$ m/s and $\alpha = 1$ . (S.E.M. is the standard error of the mean.)					
		m. biceps brachii		m. extensor carpi radialis	
		mean	S.E.M.	mean	S.E.M.
$h_{\max}$	(mm)	2.7	-	3.1	-
$h_{\min}$	(mm)	1.8	0.2	1.2	0.3
$\sigma_t$	(ms)	0.60	0.04	0.47	0.02
average error	(dB)	0.5	0.1	0.8	0.1
samples		10		6	

### Whole-Muscle Parameters

The whole-muscle signal parameters have also been identified in a number of cases [4]. The data used, a subset of the data obtained by Lindström *et al.* [27], were myoelectric signals from muscles biceps brachii *dx* and extensor carpi radialis *dx*, processed by a seven-channel octave band analyzer to yield spectra ranging from 16 to 1000 Hz. The results of one particular identification are listed in Table I. In this identification the parameter  $h_{\max}$  was given the fixed value of 5 mm and the signal source was assumed to have a power spectrum proportional to the frequency up to 1 kHz. Increased values of  $h_{\max}$  yielded slightly increased identified values of  $h_{\min}$  and  $v$ , while that of  $\sigma_t$  remained unchanged. In another parameter identification, on the same data but now with a fixed value of  $v$  (4 m/s), the results listed in Table II were obtained. The slope  $\alpha$  of the source power spectrum was also varied in a series of experiments. As in the case of changing  $h_{\max}$ , the influence due to changes in  $\alpha$  was almost negligible in the identification of values of  $\sigma_t$ . The parameters  $h_{\min}$  and  $v$  displayed the same dependence: an increase of  $\alpha$  to twice its original value reduced the identified values of  $h_{\min}$  and  $v$  to approximately half the original ones. The properties of the source are thus rather crucial in whole-muscle signal parameter identification.

In general, the parameter values found in the identification experiments agree quite well with previously reported data,

stated above. The values of  $\sigma_t$  obtained are quite stable for both motor-unit and whole-muscle signals. When comparing 6  $\sigma_t$  to experimental data, it should be noted that most definitions of duration used in clinical practice are vague. It should also be reemphasized that the assumed Gaussian density of arrival times within the motor unit quite certainly predicts too low values of  $\sigma_t$ . A rectangular density, say, yields values of  $\sigma_t$  which are 60 percent larger than those yielded by the Gaussian density. The apparently low values of  $h_{\min}$  obtained can be explained, at least in part, by excessive high-frequency content caused by background noise and other disturbances.

### APPLICATIONS

Applications of the myoelectric signal power spectrum model have theoretical as well as practical aspects. The model can be used for screening possible mechanisms to explain experimental findings. It can also be used as a guide in the design of experiments and clinical EMG routines. We shall give a few examples to illustrate possible applications.

The earliest application of the model was dip analysis, used in the study of localized muscle fatigue. It was shown [24] that sustained forceful contractions shifted the positions of the dips in whole-muscle signal spectra to lower frequencies, indicating a decrease in conduction velocity. For isometric steady contractions the course of the velocity decrease was very closely exponential with a time constant approaching 1 min for heavy loads. Dip displacements during forceful contractions were later also found in single-motor-unit signals by Broman [28], who also studied the recovery phase after the contraction.

Parameter identification of measured spectra has been mentioned. Such procedures are of great clinical importance since they yield information which is more easily related to morphological, chemical, and other causes than is the information obtained in classical EMG. Apart from its potential use in the conventional field of neuromuscular diseases, the method of parameter identification of myoelectric spectra offers the possibility of following electrolyte changes in patients with, say, renal failure, burns, and certain metabolic diseases which alter the tissue pH.

### Cross-Power Spectra

A further example of application of the model is an investigation [29] of the theoretical basis for myoelectric cross-correlation measurements. During this decade such measurements have been considered to lend the most important support to the idea of *synchronization* (or temporal grouping) of signals from different motor units. The model presented here suggests that the low-frequency components of the myoelectric signals can be propagated over long distances with only moderate damping. Expressions for the cross-correlation function were obtained by Fourier transformation of theoretical cross-power spectra of a motor-unit signal recorded at two different points with bipolar surface electrodes. The result shows that the maximum value of the cross-correlation function is monotonically increasing with the plate separation of the individual electrodes and decreasing with increasing values of the conduction velocity of the action potentials.

The general shape of the cross-correlation function depends on the conduction velocity, the motor-unit signal duration, the electrode configuration, and the observation distances. Summation of uncorrelated contributions from the whole muscle yielded an expression for the maximum value of normalized cross correlation as a function of the distance



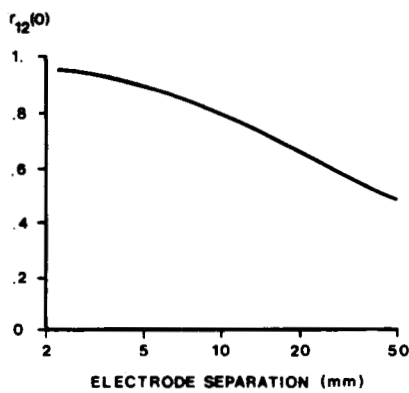


Fig. 7. Maximum value of the normalized cross-correlation function of whole-muscle signals versus the separation of the two monopolar electrodes placed on opposite sides of the muscle belly. The signals of the motor units in the muscle are nonsynchronized. Parameter values are: standard deviation of motor-unit signal temporal dispersion  $\sigma_T = 0.5$  ms and conduction velocity  $v = 4$  m/s.

between two electrodes placed on opposite sides of the muscle belly. As seen in Fig. 7, this function attains high values even if motor-unit signal synchronization is supposed not to occur.

#### Power Spectrum Moments

Power spectrum moments of various orders are of central importance in a number of applications. These moments reflect the influence of different parameters in the expressions for the myoelectric power spectrum. Moments of low order are moderately sensitive to variations in most of the parameters. Moments of increasing order increasingly emphasize the importance of parameters such as motor-unit signal duration and electrode-to-muscle distance, while the influences of muscle size and needle electrode insertion depth or bipolar electrode plate separation decrease. The action-potential conduction velocity particularly affects moments of low and high orders. Those of low order are inversely proportional and those of high order are directly proportional to some power of the velocity. Spectral moments of negative order might also be of some interest, since they are less sensitive to variations due to summation phenomena and crucial parameters such as electrode-to-muscle distance and motor-unit recruitment.

The moment of order zero, i.e., the energy of the myoelectric signal, has a variety of applications in fields such as ergonomics, functional anatomy, sports medicine, biomechanics, and prosthesis control. An expression has been derived [5], based on (27), which relates the energy of the whole-muscle signal to a number of parameters. The energy is found to increase with decreasing values of the action-potential conduction velocity, the motor-unit signal duration, and the electrode-to-muscle distance. The change of energy with velocity might offer a simple explanation of the finding [30]–[32] that the myoelectric signal strength increases during heavy contractions. The energy is also found to increase asymptotically with increasing muscle size and electrode plate separation. It is also demonstrated that, in the case of bipolar electrodes, the energy of myoelectric signals decreases as the electrodes approach the center of the innervation zone.

By normalizing the first moment  $M_1$  with respect to that of order zero  $M_0$  we find an expression which is proportional to the conduction velocity. Thus by continuously monitoring  $M_1/M_0$  during a contraction, forceful or not, we can follow the development of muscle fatigue as reflected by velocity changes [33], [34]. Recalling the experimental observation [24] that

the conduction velocity during forceful isometric contractions decreases exponentially, we perform a linear regression analysis of  $-\ln(M_1/M_0)$  versus time. The regression coefficient thus obtained is an estimate of the inverse value of the time constant characterizing the time course of the fatiguing process. The analysis can be extended to include a Student t-test of the regression coefficient being nonzero. One can thus also determine the probability of actually having fatigued muscles [33], [34].

As mentioned above, the motor-unit signal parameters (duration and number of phases) can be obtained at low levels of contraction only. It is therefore interesting to note that spectral moments of whole-muscle signals can be used at virtually any level of contraction to calculate equivalent values of duration and number of phases. Based on the zero-crossing theory of Rice [35], spectral moment analysis also reveals [36] the strong interrelation of a number of specialized time domain methods (e.g., see [37], [38]).

Other fields of application of the model for myoelectric signals are: a) prosthesis control (optimization of electrode configuration, calculation of cross talk from adjacent muscles, and estimation of the benefit of prewhitening), b) biomechanical modelling (influence of motor-unit recruitment, muscle size, and electrode placement on the relation of mechanical to myoelectrical parameters), and c) vocational medicine (interpretation of toxic effects induced by heavy metals and solvents).

#### DISCUSSION

The muscle tissue has been assumed to be electrically isotropic. Experiments indicate that the longitudinal conductivity of striated muscle is approximately 10 times larger than that in the transverse direction. Theoretically, the anisotropy can be taken into account by a coordinate transformation yielding equations for an equivalent isotropic case [39]. In this transformation, the scale factors are determined by the square root of ratios between elements in the conductivity tensor. The implication for myoelectric measurements is that *within the muscle* one finds a more rapid radial decline of the field than is stated by (2).

We have neglected the occurrence of inhomogeneities and boundaries in the muscle, e.g., large blood vessels, nerves, and bones. The most dominant influence is probably that imposed by the skin surface. This case can be treated by the superposition of mirror fields, the effect of which on surface lead-off signals is that of an essentially frequency-independent scale factor [1].

An interesting property of the myoelectric signal is its repetitive character, which causes the power spectrum to split into two parts, one discrete and the other continuous. It can be shown [40] that the mean power density, as calculated over a bandwidth equal to the average frequency of repetition, displays only minor changes due to changes in the temporal arrangement. The spectrum envelope, determined by the shape of the single signal impulse, is thus essentially preserved almost independent of variations in repetition time intervals (cf. Fig. 1). For normally distributed intervals with standard deviation  $\sigma_T$ , the relative discrete and continuous components are  $\exp(-\omega^2 \sigma_T^2)$  and  $1 - \exp(-\omega^2 \sigma_T^2)$ , respectively. As a criterion for observing lines in the composite spectrum we require the discrete component to be larger than or equal to the continuous one. With  $\sigma_T$  equal to 5–20 ms [28], [41] we find that motor-unit signal line spectra are most likely to



be seen in the low-frequency range below 15 Hz but rarely observed for frequencies higher than 50 Hz unless the signal is exceptionally regular.

The summation of motor-unit signals yields interference patterns which are occasionally interpreted as being caused by so-called synchronization of the motor-unit activities. Clinicians generally agree on the possible existence of temporal groupings of the signals in some diseases, such as poliomyelitis. Experimental findings [42] also indicate the occurrence of motor-unit synchronization as a result of special types of physical training involving brisk rapid movements of short duration. Other cases in which synchronization is said to occur are those involving forceful contractions [32], [43]–[45]. So far, the most outstanding experimental evidence of the existence of synchronized activity is that obtained from cross-correlation measurements of signals recorded over the muscle belly at two points several centimeters apart. Such experiments, yielding normalized maximum cross-correlation values in the range 0.4–0.9 [43], are generally considered to prove the occurrence of synchronization.

However, since one of the implications of the present model is that low-frequency components of myoelectric signals can propagate over long distances with low damping, high maximum values of the cross-correlation function of two separate signal derivations are likely to be observed. Synchronization of motor-unit signals is thus not a *necessary* prerequisite for the high maximum values obtained. We have therefore not included such phenomena in the model. The influence of synchronization on the whole-muscle signal power spectrum would be of the same kind as that found for the summation of single-fiber contributions.

One of the most critical points in modelling bioelectric activity is the description of the signal source. This is certainly the case in various models of myoelectricity, which are provided with sources characterized by moving dipoles or tripoles [46]–[48], exponentially declining membrane currents [46], the Gaussian form of fiber surface potentials [49], [50], etc. An attractive feature of the present power spectrum description of the signal at the source is that no particular signal shape need be assumed. The guess we have made in our model is that the action potentials, as measured at the fiber surface, have a power spectrum which over the frequency range of standard clinical interest is proportional to the frequency, i.e., that  $\alpha = 1$  in (36). This value of  $\alpha$  might be too low. In the multielectrode used in the single-fiber experiments to determine  $\alpha$ , the small electrode plates are embedded in insulating epoxy resin, which probably affects the potential recorded at the plates. There are good reasons to assume that this "wall effect" has somewhat decreased the experimentally found value of  $\alpha$ .

In many aspects the model we have presented here is far from original. It is based on the contributions of a very great number of investigators, and we apologize to the many authors we have not cited.

#### ACKNOWLEDGMENTS

The mathematical model described in this paper is a result of joint efforts in the Department of Applied Electronics, Chalmers University of Technology, and the Department of Clinical Neurophysiology, Sahlgren Hospital, Göteborg, Sweden. It is a pleasure to acknowledge the contributions and assistance of staff members in these two departments.

#### REFERENCES

- [1] L. Lindström, "On the frequency spectrum of EMG signals," *Res. Lab. Med. Electr.*, Göteborg, Sweden, Tech. Rep. 7:70, 1970.
- [2] —, "A model describing the power spectrum of myoelectric signals. Part I: Single fiber signal," *Res. Lab. Med. Electr.*, Göteborg, Sweden, Tech. Rep. 5:73, 1973.
- [3] H. Broman and L. Lindström, "A model describing the power spectrum of myoelectric signals. Part II: Motor unit signal," *Res. Lab. Med. Electr.*, Göteborg, Sweden, Tech. Rep. 8:74, 1974.
- [4] L. Lindström and H. Broman, "A model describing the power spectrum of myoelectric signals. Part III: Summation of motor unit signals," *Res. Lab. Med. Electr.*, Göteborg, Sweden, Tech. Rep. 9:74, 1974.
- [5] L. Lindström and R. Kadefors, "A model describing the power spectrum of myoelectric signals. Part IV: Total power," *Res. Lab. Med. Electr.*, Göteborg, Sweden, Tech. Rep. 10:74, 1974.
- [6] L. Lindström, "Contributions to the interpretation of myoelectric power spectra," thesis, Chalmers Univ. of Technology, Göteborg, Sweden, 1974.
- [7] R. Kadefors, P. Herberts, and L. Lindström, "On the use of fine wire electrodes in applied electromyography," in *Digest 11th Int. Conf. Medical and Biological Engineering* (Ottawa), 1976.
- [8] V. Pollak, "The waveshape of action potentials recorded with different types of electromyographic needles," *Med. & Biol. Engng.*, vol. 9, pp. 657–664, Nov. 1971.
- [9] I. Petersén and E. Kugelberg, "Duration and form of action potential in the normal human muscle," *J. Neurol. Neurosurg. Psychiatr.*, vol. 12, pp. 124–128, 1949.
- [10] F. Buchthal, C. Guld, and P. Rosenfalck, "Action potential parameters in normal human muscle and their dependence on physical variables," *Acta Physiol. Scand.*, vol. 32–33, pp. 200–218, 1954–1955.
- [11] R. Kadefors, "Myo-electric signal processing as an estimation problem," in *New Developments in Electromyography and Clinical Neurophysiology*, J. E. Desmedt, Ed. Basel: Karger, 1973, vol. 1, pp. 519–532.
- [12] R. Kadefors, A. W. Monster, and I. Petersén, "A new aspect on electrode design in myo-electric control systems," in *Proc. 8th Int. Conf. Medical and Biological Engineering* (Chicago), 1969.
- [13] F. Buchthal, C. Guld, and P. Rosenfalck, "Multielectrode study of the territory of a motor unit," *Acta Physiol. Scand.*, vol. 39, pp. 83–104, 1957.
- [14] E. Kaiser and I. Petersén, "Frequency analysis of muscle action potentials during tetanic contraction," *Electromyography*, vol. 3, pp. 5–17, 1963.
- [15] J. L. Trimble, B. L. Zuber, and S. N. Trimble, "A spectral analysis of single motor unit potentials from human extra-ocular muscle," *IEEE Trans. Biomed. Eng.*, vol. BME-20, pp. 148–151, Mar. 1973.
- [16] R. Kadefors and I. Petersén, "Spectral analysis of myoelectric signals from muscles of the pelvic floor during voluntary contraction and during reflex contractions connected with ejaculation," *Electromyography*, vol. 10, pp. 45–68, 1970.
- [17] R. Kadefors, I. Petersén, and B. Tengroth, "Quantitative analysis of EMG from m. rectus lateralis oculi," *Scand. J. Rehab. Med.*, Suppl. 3, pp. 115–120, 1974.
- [18] C. H. Häkansson, "Conduction velocity and amplitude of the action potential as related to circumference in the isolated fibre of frog muscle," *Acta Physiol. Scand.*, vol. 37, pp. 14–34, 1956.
- [19] A. L. Hodgkin and A. F. Huxley, "A quantitative description of membrane current and its application to conduction and excitation in nerve," *J. Physiol. (London)*, vol. 117, pp. 507–544, 1952.
- [20] H. Broman, L. Lindström, R. Magnusson, I. Petersén, and E. Stålberg, "Interpretation of myoelectric signal power spectra. Part II: Experimental verification," in *Digest European Conf. Electrotechnics (EUROCON'74)*, (Amsterdam), 1974.
- [21] —, "Determinants of myo-electric power spectra. Part II: Experimental verification," *Third Int. Congr. Electrophysiological Kinesiology* (Pavia, Italy), pp. 96–101, 1967.
- [22] J. Ekstedt, "Human single muscle fiber action potentials," *Acta Physiol. Scand.*, vol. 61, suppl. 226, pp. 1–96, 1964.
- [23] E. Stålberg, "Propagation velocity in human muscle fibres in situ," *Acta Physiol. Scand.*, vol. 70, suppl. 287, pp. 1–112, 1966.
- [24] L. Lindström, R. Magnusson, and I. Petersén, "Muscular fatigue and action potential conduction velocity changes studied with frequency analysis of EMG signals," *Electromyography*, vol. 10, pp. 341–356, 1970.
- [25] F. Buchthal, C. Guld, and P. Rosenfalck, "Innervation zone and propagation velocity in human muscle," *Acta Physiol. Scand.*, vol. 35, pp. 174–190, 1955.
- [26] F. Buchthal, P. Pinelli, and P. Rosenfalck, "Action potential parameters in normal human muscle and their physiological determinants," *Acta Physiol. Scand.*, vol. 32–33, pp. 219–229, 1954–1955.

- [27] L. Lindström, R. Magnusson, and I. Petersén, "Muscle load influence on myoelectric signal characteristics," *Scand. J. Rehab. Med.*, suppl. 3, pp. 127-148, 1974.
- [28] H. Broman, "An investigation on the influence of a sustained contraction on the succession of action potentials from a single motor unit," *Res. Lab. Med. Electr.*, Göteborg, Sweden, Tech. Rep. 3:73, 1973.
- [29] L. Lindström, "On cross-correlation measurements of myoelectric signals," *Res. Lab. Med. Electr.*, Göteborg, Sweden, Tech. Rep. 11:74, 1974.
- [30] S. Cobb and A. Forbes, "Electromyographic studies of muscular fatigue in man," *Am. J. Physiol.*, vol. 65, pp. 234-251, 1923.
- [31] R. G. Edwards and O. C. J. Lippold, "The relation between force and integrated electrical activity in fatigued muscle," *J. Physiol. (London)*, vol. 132, pp. 677-681, 1956.
- [32] J. Scherrer and A. Bourguignon, "Changes in the electromyogram produced by fatigue in man," *Am. J. Physical Med.*, vol. 38, pp. 170-180, 1959.
- [33] L. Lindström, R. Kadefors, and I. Petersén, "A new electromyographic index for muscle fatigue studies," in *Digest 11th Int. Conf. Medical and Biological Engineering* (Ottawa), 1976.
- [34] —, "An electromyographic index for localized muscle fatigue," manuscript submitted for publication.
- [35] S. O. Rice, "Mathematical analysis of random noise," *Bell Syst. Tech. J.*, vol. 23, 24, pp. 1-162, 1944-1945.
- [36] L. Lindström, H. Broman, R. Magnusson, and I. Petersén, "On the interrelation of two methods of EMG analysis," *Electroenceph. clin. Neurophysiol.*, vol. 34, p. 801, 1973.
- [37] M. H. Dowling, P. Fitch, and R. G. Willison, "A special purpose digital computer (BIOMAC 500) used in the analysis of the human electromyogram," *Electroenceph. clin. Neurophysiol.*, vol. 25, pp. 570-573, 1968.
- [38] A. Moosa and B. H. Brown, "Quantitative electromyography: A new analogue technique for detecting changes in action potential duration," *J. Neurol. Neurosurg. Psychiat.*, vol. 35, pp. 216-220, 1972.
- [39] P. W. Nicholson, "Experimental models for current conduction in an anisotropic medium," *IEEE Trans. Biomed. Eng.*, vol. BME-14, p. 55, 1967.
- [40] G. G. Macfarlane, "On the energy-spectrum of an almost periodic succession of pulses," *Proc. IRE*, vol. 37, pp. 1139-1143, 1949.
- [41] H. P. Clamann, "Statistical analysis of motor unit firing patterns in a human skeletal muscle," *Biophys. J.*, vol. 9, pp. 1233-1251, 1969.
- [42] H. S. Milner-Brown, R. B. Stein, and R. G. Lee, "Synchronization of human motor units: Possible roles of exercise and supraspinal reflexes," *Electroenceph. clin. Neurophysiol.*, vol. 38, pp. 245-254, 1975.
- [43] R. S. Person and L. N. Mishin, "Auto- and cross-correlation analysis of the electrical activity of muscles," *Med. Electron. Biol. Engng.*, vol. 2, pp. 155-159, 1964.
- [44] R. S. Person and M. S. Libkind, "Modelling of interference bioelectrical activity," *Biophysics (Biofizika)*, vol. 12, pp. 145-153, 1967.
- [45] O. C. J. Lippold, J. W. T. Redfearn, and J. Vuco, "The electromyography of fatigue," *Ergonomics*, vol. 3, pp. 121-131, 1960.
- [46] P. Rosenfalck, *Intra- and Extracellular Potential Fields of Active Nerve and Muscle Fibres*. København, Denmark: Akademisk Forlag, 1969.
- [47] R. E. Pattle, "The external action potential of a nerve or muscle fibre in an extended medium," *Phys. Med. Biol.*, vol. 16, pp. 673-685, 1971.
- [48] J. Ekstedt and E. Stålberg, "How the size of the needle electrode leading-off surface influences the shape of the single muscle fibre action potential in electromyography," *Computer Programs in Biomedicine*, vol. 3, pp. 204-212, 1973.
- [49] R. Plonsey, "Volume conductor fields of action currents," *Biophys. J.*, vol. 4, pp. 317-327, 1964.
- [50] J. Clark and R. Plonsey, "A mathematical evaluation of the core conductor model," *Biophys. J.*, vol. 6, pp. 95-112, 1966.

# Signal Processing for the Multistate Myoelectric Channel

PHILIP A. PARKER, JOHN A. STULLER, AND R. N. SCOTT, SENIOR MEMBER, IEEE

**Abstract**—In the multistate myoelectric channel, a single myoelectric signal source is used to control a multifunction powered prosthesis. The selection of a prosthesis function requires a receiver to process the myoelectric signal, contaminated with noise, and to decide on the basis of the received signal which function is desired. Thus the channel clearly presents a problem of choice of receiver and of decision strategy. Previous solutions to this problem have been basically empirical. In this paper we seek the optimum receiver where optimum is in the minimum probability of error sense. First a model is developed for the bipolar myoelectric signal to provide information about the relevant signal parameters and statistics. Using this information the Bayes minimum probability of error receiver is derived for an arbitrary signal parameter set. The optimum signal parameter set is then found for the Bayes receiver, and the receiver performance calculated. The receiver performance is measured and compared with the calculated performance. A significant performance improvement is seen in the optimum receiver over a more conventional receiver.

Manuscript received May 13, 1976; revised August 27, 1976. This work was supported in part by the Canadian National Research Council and the Department of National Health and Welfare.

The authors are with the Bioengineering Institute and Electrical Engineering Department, University of New Brunswick, Fredericton, N.B., Canada.

## I. INTRODUCTION

THE MYOELECTRIC channel has attracted considerable interest in the field of aids for the disabled, the most well known application being the control of powered prostheses [1], [2]. This paper deals with myoelectric signal processing for the multistate myoelectric channel.

The approach taken here is to view the human operator as a complex data gathering and processing system having various input-output information channels with which to communicate with his environment. His myoelectric channel is one in which information is conveyed to the machine via the electrical signal generated by an active skeletal muscle. A specific muscle is chosen as the signal source and a specific parameter  $\gamma$  of this signal is chosen as the information parameter. For the multistate myoelectric channel a set  $\{\gamma_i; i = 0, 1, \dots, M-1\}$ , of discrete parameter values or states is used to designate the prosthesis functions where there are  $M$  possible functions. Each function is assigned a parameter value or state which the operator produces by generating the appropriate myoelectric signal. This process, contaminated by noise, is